Available online at www.sciencedirect.com

SCIENCE DIRECT®

Thin Solid Films 468 (2004) 273–279

www.elsevier.com/locate/tsf

Use of atomic force microscopy for imaging the initial stage of the nucleation of calcium phosphate in Langmuir–blodgett films of stearic acid

Yuanjian Zhang, Ping He, Xiudong Xu, Jinghong Li*

State Key Laboratory of Electroanalytical Chemistry, Changchun Institute of Applied Chemistry, Chinese Academy of Sciences, 159 People Street, Changchun 130022, China

Received 23 September 2003; received in revised form 4 April 2004; accepted 24 June 2004
Available online 13 August 2004

Abstract

The nucleation of calcium phosphate on the substrate of steatic acid Langmuir–blodgett film at the initial stage was investigated by atomic force microscopy. Nano-dots, nano-wires and nano-islands were observed in sequence for the first time, reflecting the nucleation of calcium phosphate and the molecular arrangement of carboxylic layer. The nucleation rates perpendicular and parallel to the carboxylic terminal group were estimated from the height and diameter of the calcium phosphate crystals, respectively. And this stage was distinct from the late explosive grown stage, in which the change of the morphology was not obvious. The approaches based on this discovery would lead to the development of new strategies in the controlled synthesis of inorganic nano-phases and the assembly of organized composite and ceramic materials.
© 2004 Elsevier B.V. All rights reserved.

Keywords: Calcium phosphate; Nucleation; Langmuir–Blodgett Films

1. Introduction

The processes of biomineralization, in which living organisms form inorganic solids, are everywhere from bones and teeth to natural pearls to the small magnetic particles formed by the magnetotactic bacterial. In general, these biominerals are formed in the organic interface, which exerts the remarkable control over a crystal's size, shape, and crystallographic orientation [1–7]. Therefore, from the viewpoint of crystal growth, the interaction between organic and inorganic interface is one of the most important issue of the biomineralization. Bone is an inorganic–bioorganic composite material consisting mainly of collagen proteins and hydroxyapatite [$Ca_{10}(PO_4)_6(OH)_2$, one kind of calcium phosphates] [2,3]. The collagen proteins serve as template in the process of bone growth, in which the three dimensional organization of collagen in relation to the cell, the growth kinetics of hydroxyapatite in a physiological solution and the organic–inorganic interaction on the interface should be taken into account [5]. Given the importance of the carboxylic terminal group of organic substrate in the nucleation of biominerals, the uses of Langmuir–Blodgett (LB) film and self-assembled monolayers (SAMs) of alkainethiol on a gold substrate have provided the ideal template in an atomic scale to investigate the nucleation of biominerals in nano-scale [6,8–10]. Several studies have pointed out that oriented growth of crystalline biominerals is controlled not only by the lattice match between the two dimensional template structure and the atom positions in the biominerals crystal face grown against the template, but also by the orientation of the template terminal functional group [6]. Other mechanisms acknowledged to be important are the ability of a template to provide a boundary surface, to

* Corresponding author. Tel.: +86 431 5262243; fax: +86 431 5690851.
E-mail address: lijingh@ciac.jl.cn (J. Li).

0040-6090/$ - see front matter © 2004 Elsevier B.V. All rights reserved.
doi:10.1016/j.tsf.2004.06.153

collect cation from the solution, and to otherwise affect the local chemistry that determines the kinetics of mineralization [11]. The initial nucleation process is important for it reflects the arrangement of the template organic layer and would affect the crystal structure and the composition profoundly. Besides hydroxyapatite, there are other more soluble calcium phosphates, they are $Ca_3(PO_4)_2 \cdot nH_2O$, $Ca_8H_2(PO_4)_6 \cdot 5H_2O$, and $CaHPO_4 \cdot 2H_2O$ in the order of increasing solubility [7]. But to our knowledge, the time scale for the growth observation was too long, typically for a few days in the previous studies [5,6,8–10,12,13]. The crystalline had already grown into a few micrometers, so that it was unclear what should occur in the initial stage of the nucleation, and the related reports were few [14]. In particular, the single molecular area of LB film can be controlled easily under the proper surface pressure to satisfy the lattice match [9]. Therefore, in the present study, we use atomic force microscopy (AFM) to investigate the nucleation of calcium phosphate on the LB film of stearic acid at the initial stage for one hour or less.

2. Experimental details

2.1. Chemical

Stearic Acid (SA) was purchased from Aldrich. The spreading solvent, chloroform, was re-distillated before use. Isopropanol, $Ca(OH)_2$ and H_3PO_4 were analytical grade and were used without any further purification. All aqueous solutions were prepared with Milli-Q water (>18.2 MΩ cm^{-1}).

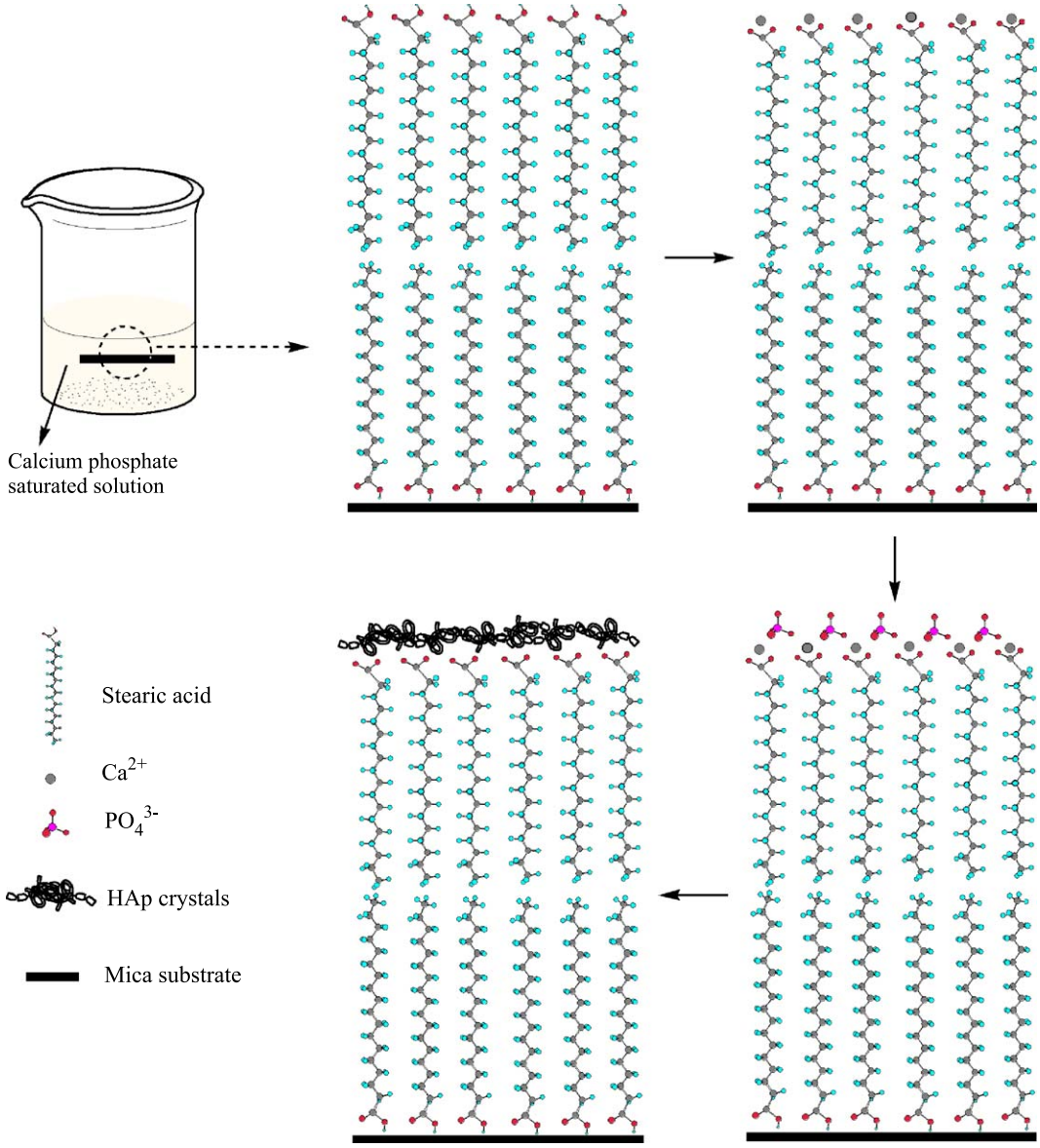

Fig. 1. Schematic representation of nucleation process of calcium phosphate.

2.2. Sample preparation

Hydrophilic substrates of a thin mica film and CaF_2 were used as substrates for the deposition of the LB films and used for atomic force microscopy (AFM) and Fourier transform infrared spectroscopy (FT-IR) measurements, respectively. The fresh mica surface was obtained by cleaving with adhesive tape. CaF_2 substrate was under ultrasonic treatment in isopropanol for 30 min. All these surfaces were completely hydrophilic after above treatment.

The SA LB films were prepared by spreading 200 μL of 1 mM chloroform solution of SA onto Milli-Q water subphase at 20 °C in a Langmuir trough with a Wilhelmy balance (KSV-5000, KSV Instrument, Finland). After waiting for 10 min to allow the solvent to be fully evaporated, the monolayer was compressed up to the target surface pressure (25 mN/m, in this case the lattice match would be satisfied) at a speed of 4 mm/min and, kept at this constant pressure for 5 min. The monolayer was then transferred to the substrates in Y-type mode at the speed of 4 mm/min by the vertical dipping method. In order to mime the double-layered bio-construction, we used two-numbered LB films with one hydrophilic surface in air (Fig. 1).

The saturated solution of calcium phosphate for crystal growth was achieved by dissolving proper fresh hydroxyapatite in water. Stiochiometric hydroxyapatite was prepared by previous published method [15]. Briefly, an ultrasonically treated 0.010 mol $Ca(OH)_2$ (aqueous solution) was titrated with 0.006 mol H_3PO_4. After aging, washing and filtration, the crude product was dried at 100 °C in vacuum.

Crystal growth of calcium phosphate on the substrate was performed by dipping the substrate in the saturated solution for different time. Then the sample was taken out quickly and the saturated solution of calcium phosphate on the surface was rinsed out of the substrate thoroughly with water. It was important to terminate the crystal growth in the latter step. Considering the relatively slow scanning speed of AFM probe, the observation *in situ* at very initial stage was not likely possible. Therefore, in the present study, the terminal process of crystal growth and the *ex situ* observation were adopted.

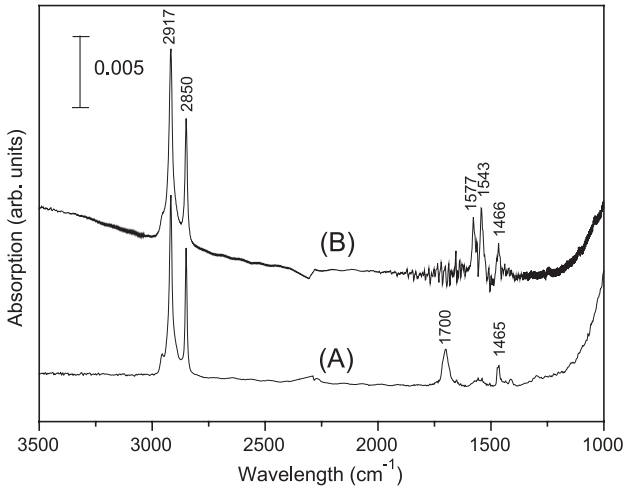

Fig. 2. FT-IR spectra of the stearic acid LB films (A) before and (B) after soaking in calcium phosphate saturated solution for 30 min.

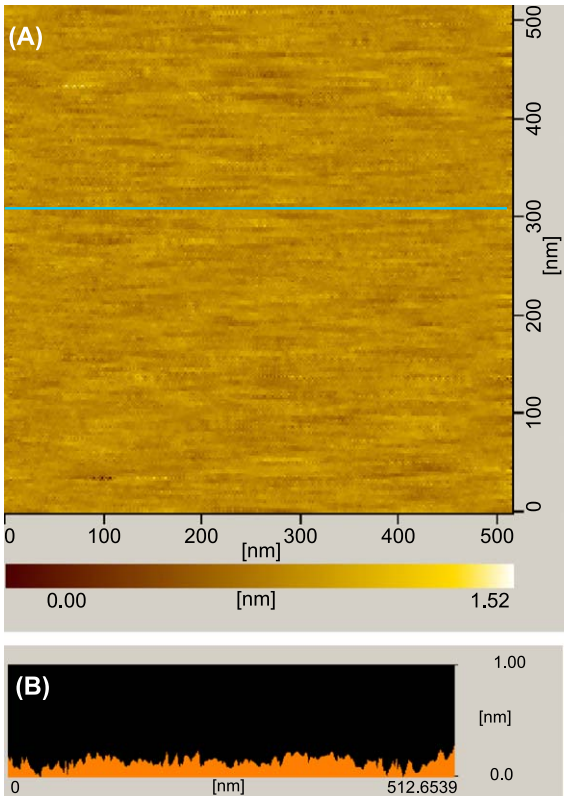

Fig. 3. (A) AFM Topographic image of two-numbered stearic acid LB films on the mica. (B) Cross-section analysis of the line in A.

2.3. Instruments

Fourier transform infrared spectroscopy was conducted at FTS135 infrared spectroscopy (BIO-RAD, USA). Absorption spectrum (FT-IR) of the SA LB films before and after soaking in the calcium phosphate saturated solution (30 min) was obtained on the CaF_2 substrate.

The surface topographies of the samples were investigated using an optical beam deflection commercial AFM system (SPA400 multifunction unit/SPI3800 probe station, Seiko Instruments, Japan) operated in the ambient atmosphere. A rectangular gold-coated silicon cantilever, cleaned by the UV treatment, was employed with its normal force constant, resonance frequency and Q factor being 1.6 N/m, 24.58 kHz and approximately 180, respectively. The cantilever was vibrated at a frequency of 24.25 kHz, slightly lower than the resonant frequency of the cantilever. Topographic images of the samples were acquired at a probe scan rate of 0.5 – 1.0 Hz.

3. Results and discussion

When the carboxylate-functionalized LB films were introduced into calcium phosphate saturated solution, a counterion overlayer was formed by bonding of the Ca^{2+} ions to the carboxylate group on the LB films, which also fixed the position of the carboxylate functionalities on the LB films. Then the formation of the counterion layer started the nucleation process by attracting the free PO_4^{3-} and OH^- ions in solution as illustrated in Fig. 1 [6,12]. In this process, the slight structural change of SA could be measured by FT-IR. Fig. 2A shows the FT-IR spectrum of SA LB films, in which the strong peaks at ca. 2917 and 2850 cm^{-1} were assigned to the antisymmetric and symmetric CH_2 stretching vibrations of the SA hydrocarbon chains, respectively [16]. And the peaks at ca. 1700 and 1464 cm^{-1} were assigned to the stretching mode of the C=O in a carboxylate group and scissoring vibration of CH_2, respectively [16]. When the nucleation process started, the peak at 1700 cm^{-1} disappeared while the antisymmetric COO^- stretching vibrations peaks correspondingly appeared at ca. 1577 and 1543 cm^{-1} (Fig. 2B) [16,17]. It indicated that the hydrogen ions were dissociated from carboxylate group and then the Ca^{2+} ions were absorbed on it. Moreover, the sequent nucleation of calcium phosphate was expected to occur, for if only Ca^{2+} ions exchanged with hydrogen ions, the peak of symmetric C=O stretching vibration at ca. 1700 cm^{-1} would appear , as Tanaka et al. pointed out. They investigated the FT-IR spectra of arachidic acid LB monolayers soaking (1) in $CaCl_2$ / or NaCl solution, (2) in $CaCl_2$ and subsequently in K_2HPO_4 solution, and (3) in simulated body fluid. They found that the peak of C=O at ca. 1700 cm^{-1} still appeared in the case (1), while the peaks of C=O only appeared at ca. 1576 and 1543 cm^{-1} both in the case of (2) and (3) [17]. The nucleation of calcium phosphate led to the formation of low site symmetry.

The topographic image of two-numbered SA LB films on the mica is shown in Fig. 3A. Very flat terraces were

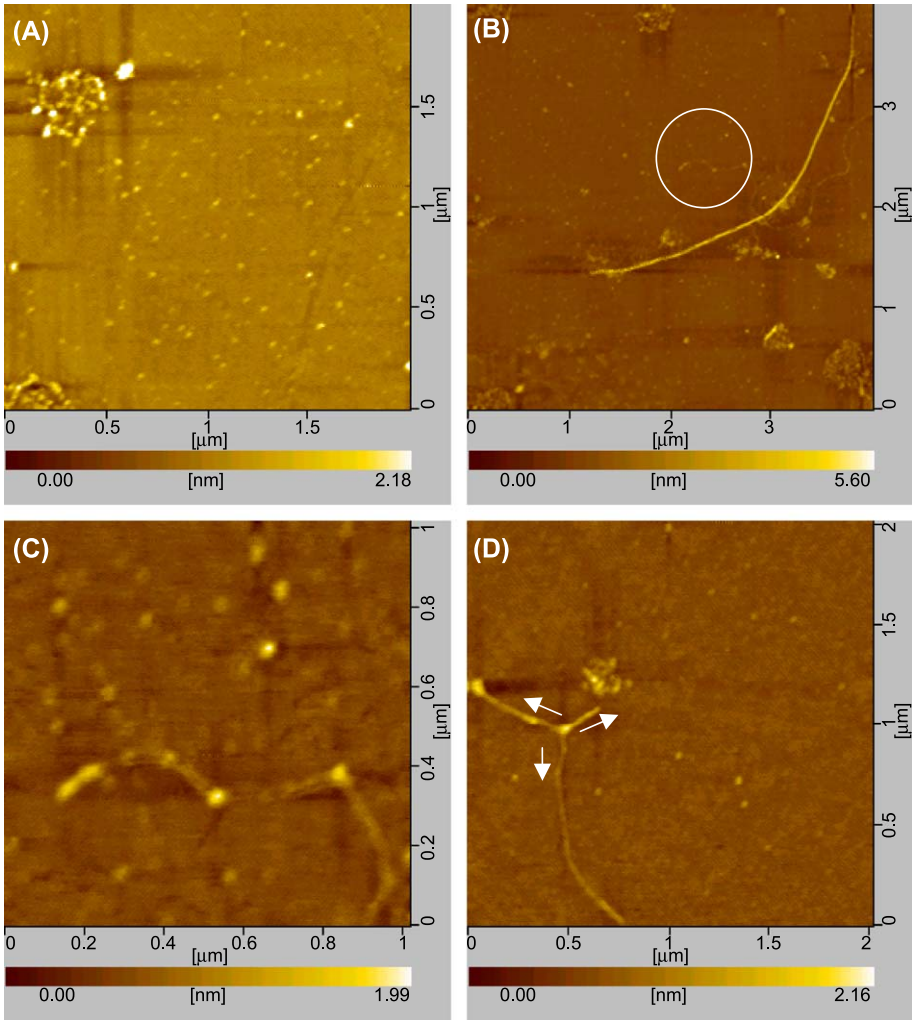

Fig. 4. AFM topographic images of the nucleation on the stearic acid LB films for 2 min. (A) Nano-particles were arranged randomly with the diameter of ca. 20–30 nm and the height of ca. 0.3–0.5 nm. (B) Nano-wires. (C) Magnified image of white circle part in (B), nano-dotted wire. (D) Coalesced nano-wires. The white arrow indicates the grown direction. The angle between any two directions was ca. 120°.

observed and only a limited number of pinholes were visible on the mica surface, suggesting LB films with a high quality were achieved [18]. The quality of the films could also be estimated with the aid of the cross-sectional analysis (Fig. 3B). The maximum height difference of the grown SA layer was only several angström, which was comparative to that of mica substrate. For the transferring ratio of both two SA layer was very close to 1, the layers was expected to cover the entire substrate, which would result in the uniform topographic image.

Fig. 4 shows the images of the nucleation for 2 min. It was found that the nano-particles were arranged uniformly with the diameter of ca. 20–30 nm and the height of ca. 0.3–0.5 nm in Fig. 4A. And some islands due to the

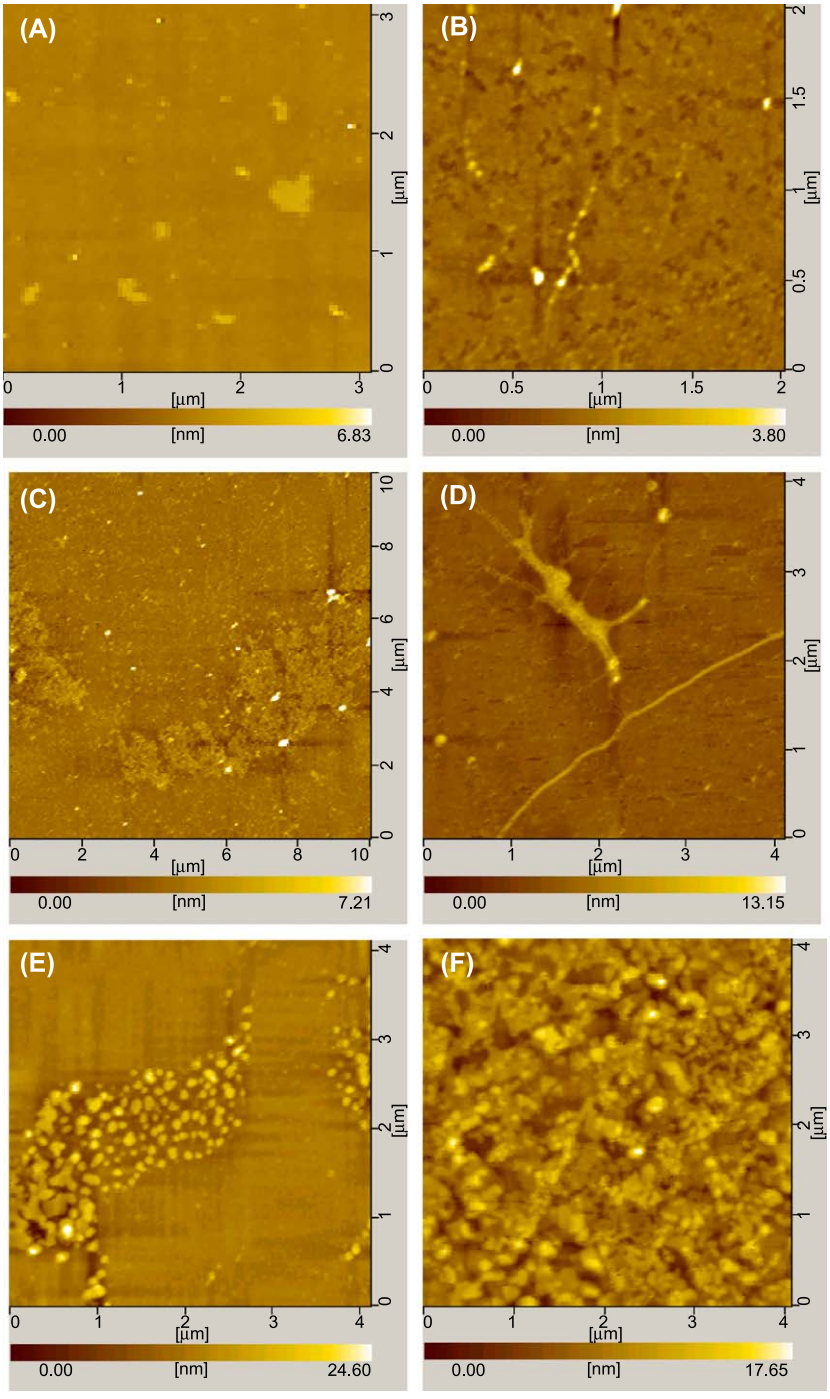

Fig. 5. AFM topographic images of the nucleation on the stearic acid LB films for 5–60 min. For 5 min more, (A) nano-islands and (B) nano-dots were observed. As the growth period increased to 10 min, larger (C) nano-islands and (D) nano-wires were formed. (E) When the growth period increased further to 30 min the nano-particles which congregate into island became larger. (F) Grown for 60 min the entire film was covered with calcium phosphate nano-crystals. The surface became rather rough.

coalescence of single nano-particles were also observed, which indicated that some isolated neighbored nano-particles grown in opposite directions and joined together later. If this growth mode occurred among linear isolated neighbored nano-particles, the nano-wire was expected to form. We did observe this phenomenon in the present study, which is shown in Fig. 4B. The partially formed nano-wire (dotted wire) indicated by the white circle part in Fig. 4B is illustrated in the magnified images (Fig. 4C). It confirmed the above supposition clearly. The direction of the arrangement was not apparent, but the trend to pack hexagonally was observed. In Fig. 4D, the apparent directions of the growth were observed, as indicated by white arrows in the figure. The angle between any two directions was ca. 120°.

As the growth period increased to 5 min, more islands were observed (Fig. 5), and the dotted wire was also observed (Fig. 5B). Multiple two-dimensional nucleations occurred on the substrate and the arrangement became more irregular. As the growth period increased further (10 min), large area of islands and wires, which were due to the coalescence of single nano-particles, were found, as shown in Fig. 5C and D. When the nucleation time reached 30 min, the islands of larger nano-particles were formed (Fig. 5E). And after 60 min, the entire substrate was covered with the nano-particles, and the surface was uniform macroscopically (Fig. 5F).

The growth rate of the calcium phosphate on the SA LB films could be estimated by measuring the change of height and diameter of the nucleation particles by cross-sectional analysis. Fig. 6A shows calcium phosphate nano-particles after 2-min nucleation. In the cross-sectional analysis (Fig. 6B) of the vertical line in the Fig. 6A, the heights of the three isolated particles (ΔZ) were calculated as 0.66, 0.50 and 0.56 nm, respectively; and the diameters were calculated as 29.9, 22.7, and 25.1 nm, respectively. The same measurement procedure was repeated in random site several times until the number of the counted particles reached 20. The same samples were used for all measurements. And all results were included in the error bars in Fig. 6C and D, except that of 60 min for the difficult statistics in this case. It was indicated that the height of the nano-particles did not change linearly with time despite the relative constant concentration of the calcium phosphate solution. There was a flat region before 10 min and a explosive increase after that (Fig. 6C). The diameter of the nano-particles increased with time nonlinearly, too. It reached the maximum at 30 min. Moreover, the turning point also appeared at ca. 10 min (Fig. 6D).

Therefore, the nucleation of calcium phosphate at the initial stage on the substrate of SA LB film could be classified into two different steps. In the former step (<10 min), calcium phosphate nano-particles were ranged in two dimension uniformly, and when the isolated nano-dots

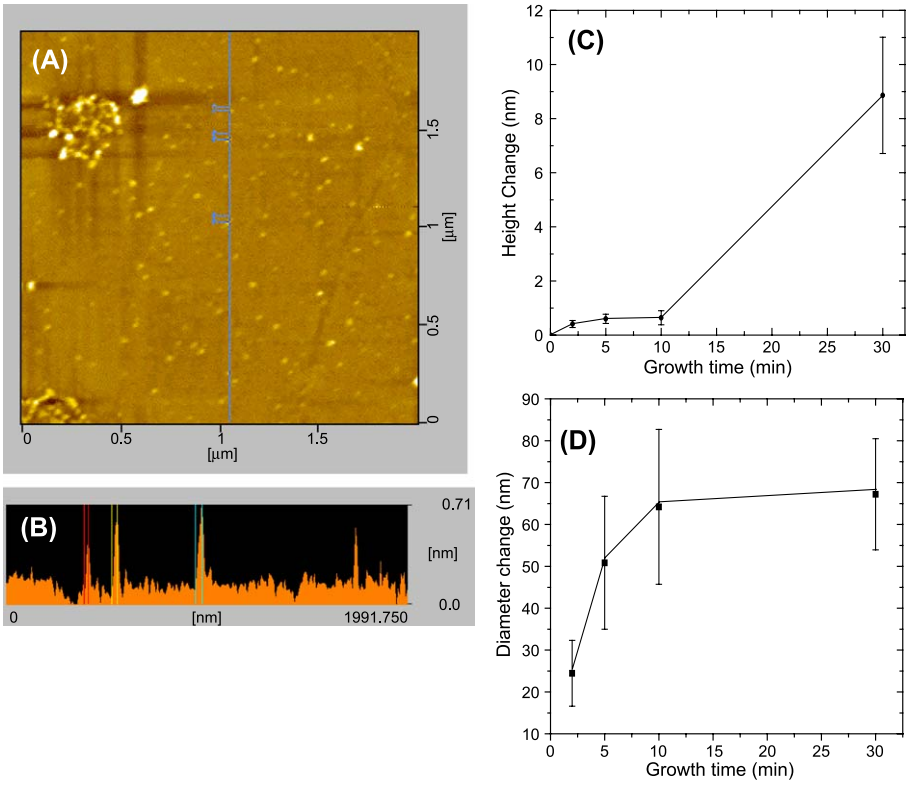

Fig. 6. (A) AFM topographic images after growth for 2 min. (B) The cross-sectional analysis indicated the height change along the line in (A). ΔZ and the distance were the relative height and diameter of the corresponding particles. (C) Relationship between the height of calcium phosphate and the grown time. (D) Relationship between the diameter of calcium phosphate and the grown time.

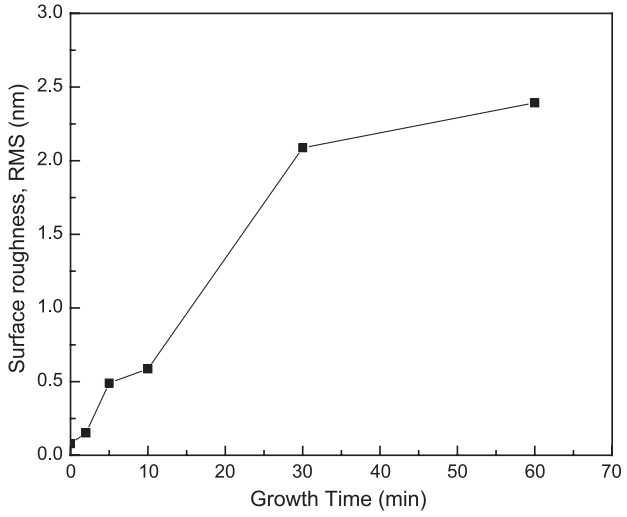

Fig. 7. The nonlinear relationship between surface roughness (estimated by root mean square) and growth time.

coalesced, nano-wires and nano-islands were observed with time. The growth perpendicular to the carboxylate surface was not obvious (ca. 0.6 nm, comparative to the height of one layered Ca^{2+}–PO_4^{3-} if linear binding between ions occurred or the diameter of one Posner cluster [19], $Ca_9(PO_4)_6$), while the nucleation parallel to the surface dominated in this step, and the entire surface was gradually covered in this period. This step might correspond to the process of fluctuation nucleation and nucleus growth. In the latter step, the growth rate was time-dependent and the whole surface was covered with calcium phosphate crystals. Only this step was described in the previous reports [12]. This process could also be estimated by the change of the surface roughness. In AFM, the surface roughness was often characterized as root mean square (RMS). Fig. 7 shows the nonlinear relationship between the RMS and different growth time. The same samples were used for all measurements. It was found that the surface roughness increased at first, and then gradually converged to constant, which corresponded to the initial nucleation and the later growth process, respectively. Characterization of calcium phosphate directly was difficult because the amount of the grown layer was too little at the initial stage, but the layer was expected to be calcium phosphate and the Ca/P ratio was higher at the former step [14]. And the different morphologies of calcium phosphate appeared in the initial stage of the nucleation might be due to the slight micro-environment differences, such as defects.

4. Conclusion

The nucleation of calcium phosphate on the substrate of stearic acid LB films at the initial stage (<1 h) was observed by AFM. It was found that the nano-dots randomly formed initially, and coalesced into the late nano-wires and nano-island. This stage was distinct from the late roaring grown stage, in which the change of the morphology was not obvious. The approaches based on this discovery would lead to the development of new strategies in the controlled synthesis of inorganic nano-phases, and the assembly of organized composite and ceramic materials.

Acknowledgement

This work was financially supported by Outstanding Youth Fund (No. 20125513) from the National Natural Scientific Foundation of China, 100 People Plan from Chinese Academy of Sciences and 100 Outstanding Ph D. Thesis Award of China.

References

[1] S. Mann, D.D. Archibald, J.M. Didymus, T. Douglas, B.R. Heywood, F.C. Meldrum, N.J. Reeves, Science 261 (1993) 1286.
[2] J.D. Hartgerink, E. Beniash, S.I. Stupp, Science 294 (2001) 1684.
[3] T.A. Taton, Nature 412 (2001) 491.
[4] R.F. Service, Science 294 (2001) 1635.
[5] J. Küther, G. Nelles, R. Seshadri, M. Schaub, H.J. Butt, W. Tremel, Chem. Eur. J. 4 (1998) 1834.
[6] Y.J. Han, J. Aizenberg, Angew. Chem. Int. Ed. 42 (2003) 3668 (and therein).
[7] S. Koutsopoulos, Langmuir 17 (2001) 8092.
[8] A.M. Travaille, J.J. Donners, J.W. Gerritsen, N.A. Sommerdijk, R.J. Nolte, H. Kempen, Adv. Mater. 14 (2002) 492.
[9] H. Unuma, K. Ito, T. Ota, M. Takahashi, J. Am. Ceram. Soc. 79 (1996) 2474.
[10] A.M. Travaille, L. Kaptijn, P. Verwer, H. Hulsken, J.A. Elemans, R.J. Nolte, H.V. Kempen, J. Am. Chem. Soc. 125 (2003) 11571.
[11] E. Dimasi, V.M. Patel, M. Sivakumar, M.J. Olszta, Y.P. Yang, L.B. Gower, Langmuir 18 (2002) 8902.
[12] C. Damle, A. Kumar, S.R. Sainkar, M. Bhagawat, M. Sastry, Langmuir 18 (2002) 6075.
[13] C.L. Ma, H.B. Lu, L.F. Wang, L.F. Zhou, F.Z. Cui, F. Qian, J. Cryst. Growth 173 (1997) 141.
[14] K. Onuma, A. Oyane, T. Kokubo, G. Treboux, N. Kanzaki, A. Ito, J. Phys. Chem., B 104 (2000) 11950.
[15] Y.J. Zhang, L.H. Zhou, D. Li, N.C. Xue, X.D. Xu, J.H. Li, Chem. Phys. Lett. 376 (2003) 493.
[16] X.Z. Luo, Z.Q. Zhang, Y.Q. Liang, Langmuir 10 (1994) 3213.
[17] K. Sato, Y. Kumagai, J. Tanaka, J. Biomed. Mater. Res. 50 (2000) 16.
[18] S. Ye, H. Noda, S. Morita, K. Uosaki, M. Osawa, Langmuir 19 (2003) 2238.
[19] K. Onuma, N. Kanzaki, A. Ito, T. Tateishi, J. Phys. Chem., B 102 (1998) 7833.